Prediction of segregation in funnel and mass flow discharge

Davide Bertuola, Silvia Volpato, Paolo Canu, Andrea C. Santomaso[*]

APTLab - Advanced Particle Technology Laboratory, Department of Industrial Engineering, University of Padova, via Marzolo 9, 35131 Padova, Italy

[*]corresponding author: Andrea C. Santomaso e-mail: andrea.santomaso@unipd.it

Abstract

In this paper we present a model to predict the onset and evolution of segregation during the discharge of binary mixtures of granular materials. The model accounts for the multi-phase and multi-component nature of the granular mixtures, to simulate the main flow regimes occurring in the discharge of silos (funnel and mass flow) and how they affect segregation. The new comprehensive model for segregation follows a continuum Eulerian approach and results from the coupling between an *ad-hoc* rheology for granular flow and a percolation model for multi-component mixtures. Predictions are compared with independent literature experimental data, for short and tall silos and prove to be quite accurate, after a tuning of the percolation flux sub-model. The larger segregation in short flow paths with smaller amount of fines reported by the experiments is quantitatively predicted. The model also predicts the three phases observed in experiments during the discharge of tall silos.

Keywords: dense granular flow; rheology; segregation modeling; silo discharge; mass flow; funnel flow.

1. Introduction

Several industries process granular materials routinely, including chemical, food and pharmaceutical to mention a few. Often, granular solids are mixtures of particles, differing in size, shape, density and other features. Because of these differences, the homogeneity of the granular mixtures can be compromised by segregation during handling operations. Segregation is the tendency of particles with different physical properties to separate from the mixtures; it can be determined by several mechanisms: sterical, inertial, frictional and related to local velocity gradients. Segregation may induce a degree of heterogeneity in the powders incompatible with the industrial process requirements or with the final products quality standards. The development of tools for prediction of segregation helps to control and minimize its occurrence and impact.

Segregation onset and drawbacks are well known in the industrial practice since a long time; notwithstanding several studies, segregation remains an open issue.

One of the oldest studies in the literature (Brown, 1939) considers a free surface flow on inclined chutes. Brown suggests that the main mechanism of segregation is the inter-particle

collisions, which cause deceleration of small particles and their concentration close to origin of flow, whereas larger particles concentrate at the end of the chute. Later, Williams (1963) suggests that inter-particle percolation is the main mechanism. Still studying free-surface flows, he observes small particles travelling through the voids on the surface, whereas large particles roll down the surface without any chance to percolate into the smaller voids. Savage and Lun (1988) also consider the inclined chute; they model the granular material as several moving layers under shear and that segregation is caused by percolation through voids and by particle migration from one layer to another. Bridgwater (1994) shows that there are three fundamental mechanisms of segregation on free flowing granular materials, which are inter-particle percolation and particle migration, occurring in the bulk, and a free surface segregation. Tapping and vibrations are also studied. Barker and Mehta (1993) conclude that segregation is driven by convection and diffusion, while Knight *et al.* (1993), through uniaxial vibration experiments, suggest that the principal segregation mechanism is convection. Gray and Thornton (2005) formulate a theoretical model to describe the segregation in free surface flow. The model is based on a simple percolation idea, in which the segregation velocity is explicitly dependent on gravity and Marks *et al.* (2011) include a time dependent shear rate contribution. These models predict a minimum distance from the feeding point beyond which a complete separation of small particles from large particles occurs.

Also Fan *et al.* (2014) develop a segregation velocity that depends on the shear rate. For Hajra *et al.* (2012) , instead, the segregation velocity depends on the particle diameter ratio. Dolgunin *et al.* (1998) develop a model for the rapid granular flow which is a sum of three contributions: convection, quasi-diffusion and segregation.

Different geometries were studied in the literature, focussing on model arrangements, such as rotating drums, chutes, vibrating vessels (Santomaso *et al.*, 2004, 2006; Taberlet *et al.*, 2006; Shi *et al.*, 2007; May *et al.*, 2010; Hajra *et al.*, 2012; Fan *et al.*, 2014). Still, the most common configuration, in the industrial processing of granular materials and powders, is the silo, with a converging hopper at discharge.

To model the flow of granular materials, a discrete or a continuum approach can be chosen. In the first, known as DEM (Discrete Element Method), forces balance is applied at each particle (Cundall *et al.*, 1979). DEM can provide detailed information about the micro-mechanics of granular material on a local scale. DEM remains limited in simulating full scale industrial equipments because of the computational costs.

 Alternatively, a continuum approach can be used (Savage 1988), in which the granular material is considered like a pseudo-fluid with a peculiar rheology. Christakis *et al.* (2002, 2006) investigate silo segregation through continuous models. The model is applied to the discharge of a binary mixture (60% of fines and 40 % of coarse) from a mass flow silo and funnel flow silo and to the discharge of ternary mixture to a funnel flow silo. The velocity of segregation is considered as the sum of three contributes: velocity due to diffusion, velocity induced by shear and velocity by percolation. The percolation term depends on the particles diameter, on the available void in the control volume and on the gravity vector, allowing the material to move and percolate even when the material do not flow.

Here, we extended a previously developed hydrodynamic model (Artoni *et al.* 2009), to predict segregation. The model was successfully used to simulate the granular flow of mono-dispersed mixtures in full industrial scale reactors and silos (Artoni *et al.*, 2011; Volpato *et al.*, 2014). The continuous model for granular flow is here combined with single species transport equations, to describe the changes in granular material composition due to segregation. Since segregation is

strongly connected with the free surface displacement, a convective equation for air is included in the comprehensive model, to track the air/pseudo-continuous granular material interface. Two types of flow regimes in silos are studied: funnel and mass flow. These determine different segregation patterns and intensity, as demonstrated by Sleppy and Puri (1996) in their experiments on sugar mixtures. The experiments by Ketterhagen *et al.* (2007) and Arteaga and Tüzün (1990) nicely prove that the funnel flow regime promotes segregation, at the discharge point, whereas mass flow regime keeps segregation bounded. These experiments were used to critically evaluate our model predictions and to assess its reliability on different scales and geometries.

2. Model outline

2.1 A comprehensive model of segregating granular flow with a free surface

The simulation of bi-dispersed granular flows, allowing for a free, moving surface was achieved by an Eulerian, continuum approach to the two phase flow. Accordingly, the static computation domain included two regions, accounting for the air and the solids, the latter treated as a pseudo-fluid with *ad-hoc* rheology. The extension and movement of the two regions were tracked by means of their interface.

The local pressure, p, and velocity field, u, were determined by the conservation equations, applied to the total mass and the momentum, for incompressible fluids:

$$\nabla \cdot u = 0 \tag{1}$$

$$\rho\left(\frac{\partial u}{\partial t} + u \cdot \nabla u\right) = -\nabla p + \nabla \cdot \left[\eta\left(\nabla u + (\nabla u)^T\right)\right] + \rho g \tag{2}$$

The local density, ρ, and viscosity, η, were very different in the air and solids domains. The values used in the unique momentum balance were determined as

$$\rho = \rho_a + (\rho_g - \rho_a)\phi \qquad \eta = \eta_a + (\eta_g - \eta_a)\phi \tag{3}$$

where the volumetric fraction of solids, ϕ, was used and the subscripts a and g indicate respectively the air and the granular material. It determined the extent of the solid domain, treated as a non-porous pseudo-fluid. For numerical stability ϕ was treated as a continuous variable which changed from 0 (air) to 1 (solid) in a very limited layer of finite thickness at the interface between the two phases. It was determined by the convective equation for a passive scalar:

$$\nabla \cdot u = 0 \tag{4}$$

This approach to two phase flow is referred to as Level Set method (Olsson and Kreiss, 2005). It allows tracking the interface motion. Its implementation may require the addition of a small, artificial diffusion flux, to cope with the sharp discontinuity at the interface, Γ.
The densities of air and of granular material, as well as the viscosity of air, were assumed constant. The local viscosity of the granular pseudo-fluid was the key to determine its movement. It was defined through a sub-model, detailed in Artoni *et al.* (2009), based on a non-local rheology (Hennan *et al.*, 2013). Shortly, the local viscosity was determined by the local granular temperature, θ, defined as the mean square fluctuating velocity (Jenkins and Savage, 1983), as:

$$\eta_g = \eta_0 \rho_g d_g^2 \exp\left(\frac{\theta^*}{\theta}\right) \tag{5}$$

where η_0 is the viscosity coefficient parameter, θ^* is a granular temperature scale, d_g is the average particle diameter and θ is the granular temperature. The granular temperature scale θ^* depends on the diameter of the particle and it is defined as $\theta^* = k_\theta \, g \, d_g$ where k_θ is a dimensionless parameter.

θ can be considered as a measure of the local mobility of the particles and calculated through the translational kinetic energy balance:

$$\frac{3}{2}\rho\frac{\partial \theta}{\partial t}+\frac{3}{2}\rho u \cdot \nabla \theta = -\Pi : \nabla u - \nabla \cdot q^T - z^T \tag{6}$$

where Π is the deviatoric stress tensor, q^T is the fluctuating energy flux and z^T is the dissipation rate.

The simulations of segregation required specifying the local fraction of different species. In this study we focused on bi-dispersed mixtures of solids, where the size was the only feature that differentiated the species. The local mass fraction of species i in the mixture, ω_i, was given by:

$$\frac{\partial \omega_i}{\partial t}+u \cdot \nabla \omega_i = \left(\nabla \cdot J_{s,i}\right)_y \qquad\qquad i=f \text{ (fines)}, c \text{ (coarse)} \tag{7}$$

that assumed a convective-segregating transport mechanism, where the segregating flux, J_s, described the separation of fines from coarse material caused by percolation; it acted in the direction of gravity (Christakis *et al.*, 2005), assumed to be *y*. We then neglected the segregation flux in *x* direction. The model was an original combination of literature models (Fan *et al.*, 2014; Hajra *et al.*, 2012). The particle diameter ratio, used by Hajra *et al.*, 2012 , and the shear rate used by Fan *et al.* (2014), were considered as the two most important factors in the percolation mechanism. The segregation velocity of small particles was assumed as:

$$v_{s,f}=-K \, d_c \left(1-\omega_f\right)\left(\frac{d_f}{d_c}-1\right)|\dot{\gamma}| \tag{8}$$

where $|\dot{\gamma}|$ was the magnitude of the shear rate, d_f and d_c the small and the large particle diameter, respectively. *K* was a model parameter discussed later.

Hajra *et al.* (2012) develop their model assuming that the segregation velocity is proportional to the difference between the diameter of small (the segregating particle) and the average diameter:

$$v_s=-K\left(d_f-\langle d\rangle\right)$$

The average diameter *<d>* is the mass averaged particle size defined as:

$$\rho=\rho_a+\left(\rho_g-\rho_a\right)\phi$$

Expanding *<d>*, the term contained in (8) is obtained. Hajra *et al.* (2012) state that the segregation velocity of each specie is proportional to the concentration of the other specie as previously found also by Savage and Lun (1988). This dependence is in agreement with the physical evidence that percolation of a fine particle increases when larger amount of coarse particles surround it because larger inter-particle void are available.

Fan *et al.* (2014) introduce in the segregation velocity, the dependence on the shear rate, since percolation occurs when the material is dilated due to flow. With the increasing of the shear rate, larger inter-particle voids are created and fine particles can percolate more easily.

This is however a necessary condition for percolation but not a sufficient one. It is also required a sufficient difference between the size of coarse and fine particles according to Hajra et al. (2012) model. The combination of the two conditions was obtained in the present percolation model through the product of the two independent sources of segregation proposed by Fan et al. (2014) and Hajra et al. (2012) respectively. It has to be considered just as a first attempt to tackle a complex phenomenon using an hydrodynamic continuum rheology in a two phase unsteady system (solid

and air) where the solid phase is a binary mixture of particles (coarse and fine). Further refinements may indeed include inertial effects occurring in the free surface flows and segregation flux in the x direction.

The segregation flux was obtained as the product between the segregation velocity and the mass fraction of small particles, as:

$$J_{s,f} = -K d_c \omega_f (1 - \omega_f) \left(\frac{d_f}{d_c} - 1 \right) |\dot{\gamma}| \tag{9}$$

and $J_{s,c} = -J_{s,f}$.

According to eq. (9), percolation does not occur in the absence of bulk deformation, differently from the model of Christakis *et al.* (2002). The solution of eq. (7) may require some artificial diffusion for convergence, particularly when sharp composition differences arise locally. It has no physical meaning, nor quantitative relevance; and it is a purely numerical artefact. All the model eqs. (1), (2), (4), (6), and (7) have the general structure of n-dimensional, advection and diffusion conservation equations, whose generalized numerical solution is implemented in several commercial and open source codes, using state-of-the-art numerical methods, and versatile pre- and post-processors to manage complex geometries. We based our implementation of the model equations on COMSOL Multiphysics (ver. 4.3), an established, wide spread FEM code that is flexible enough to implement the granular flow model. The individual species transport equation was implemented through a general coefficient form for PDEs. Note that eqs. (6) and (7) were solved only in the solids region, according to the indication of ϕ.

2.2 Initial and Boundary Conditions

The initial configuration assumed zero velocity everywhere, a specified partitioning of the domain between air and granular material (better specified in each example, see Figures 1 and 2) and a given distribution of fines consisting of a uniform initial concentration at a specified mass fraction.

Boundary conditions for eqs. (1) and (2) were the following: atmospheric pressure on the open top of the silo, slip at the walls where there was air and partial slip where the granular material was flowing. The partial slip condition at the wall set the ratio of the tangential velocity to its gradient in the normal direction, by means of a constant slip length (Artoni *et al.*, 2009). It allowed for a limited tangential velocity at the walls, as common in granular flow in contact to many comparatively smooth solid surfaces. At the silos discharge point, the flow rate was fixed, as common in industrial practice where rotary, screw or belt feeders withdraw material at a constant mass flow rate. This was simply expressed as a constant, plug flow velocity at the outlet. Among several options, depending on the extractor, in our computations we set the outlet velocity according to the Beverloo's equation (Neddermann, 1992), valid for gravity discharge of granular materials through an orifice.

Two different flow rates were imposed at the outlet: $2.2 \cdot 10^{-5}$ m^3/s for the funnel flow silo and $1.5 \cdot 10^{-4}$ m^3/s for the mass flow silo.

Boundary conditions for the phase variable ϕ were no flux at the walls and $\phi=0$ (for numerical reason the value is not equal to 0, but it is a very small number, i.e 10^{-29}) at the inlet boundary. For the translational kinetic energy, insulation was imposed at the walls whereas at the open top boundary a constant granular temperature was set, with a value equal to the average temperature of

the cylindrical part.

Mass fractions, ω_i, were bounded by a condition of zero orthogonal flux across the walls and convective flux at the outlet.

2.3 Model parameters

Viscosity of the granular, pseudo-fluid is a function of the particle diameters. In our case the two species differed just by the size, so that an average particle diameter was used. The parameters in the rheological model were calibrated so that a unique set predicted both the mass and funnel flow, depending on geometry. We used k_θ equal to 100 and η equal to 0.2. The most relevant parameter was factor K in the segregation velocity, eq. (8). As a first attempt, a constant value of K was assumed. It was however clear from comparison with experimental data that a K dependent on the composition could give better results. Hajra *et al.* (2012) indeed assume that the parameter K has both an intrinsic and a concentration-dependent component (K_T and K_S, respectively) that can be considered a complex functions of granular temperature, local void fraction, gravity, particle sizes, density, shape, roughness, coefficient of friction and coefficient of restitution. They suggest:

$$\eta = \eta_a + (\eta_g - \eta_a)\phi \tag{10}$$

i.e. a linear dependence on the fine mass fraction. The parameters in eq. (10) were tuned on the experimental data and the same values used for all the simulations done.

3. Reference experimental studies

The granular flow model accounting for segregation presented above was tuned and validated with experimental data from literature. Two sets were used, reflecting quite different silo geometry. Ketterhagen *et al.* (2007) report data in short silos, while Arteaga and Tüzün (1990) carry out measurements in tall silos. They all use binary mixtures of the materials as reported in Table 1.

Table 1. Properties of materials used in the experiments from literature.

Material	Ketterhagen *et al.* (2007)			Arteaga and Tüzün (1990)	
	Glass beads			Acrylic granules	Radish seeds
Size (µm)	521	1160	2240	605	2410
Bulk density (kg/m³)	1450			600	

3.1 Experimental studies on short silos

Ketterhagen *et al.* (2007) perform their experiments in silos with dimensions dictated by ASTM D 6940-03 standard. The cylindrical part of their silos is very short so that they mainly evaluate the amount of segregation occurring in the hopper. This is consistent with the purpose of the standard, because segregation develops mostly in the hopper, where the shear rate is higher. A larger hopper also enhances the shear dependence of the segregation flux in eq. (8), as in Hajra *et al.*, (2012).

Ketterhagen and co-worker (2007) use two transparent, acrylic silos, quite short, with very different hoppers to achieve distinct discharge regimes. They are reported in Figure 1, with the original dimensions. One operates in funnel flow (Figure 1a) while mass flow regime prevails in the taller (Figure 1b), with a longer, slender hopper.
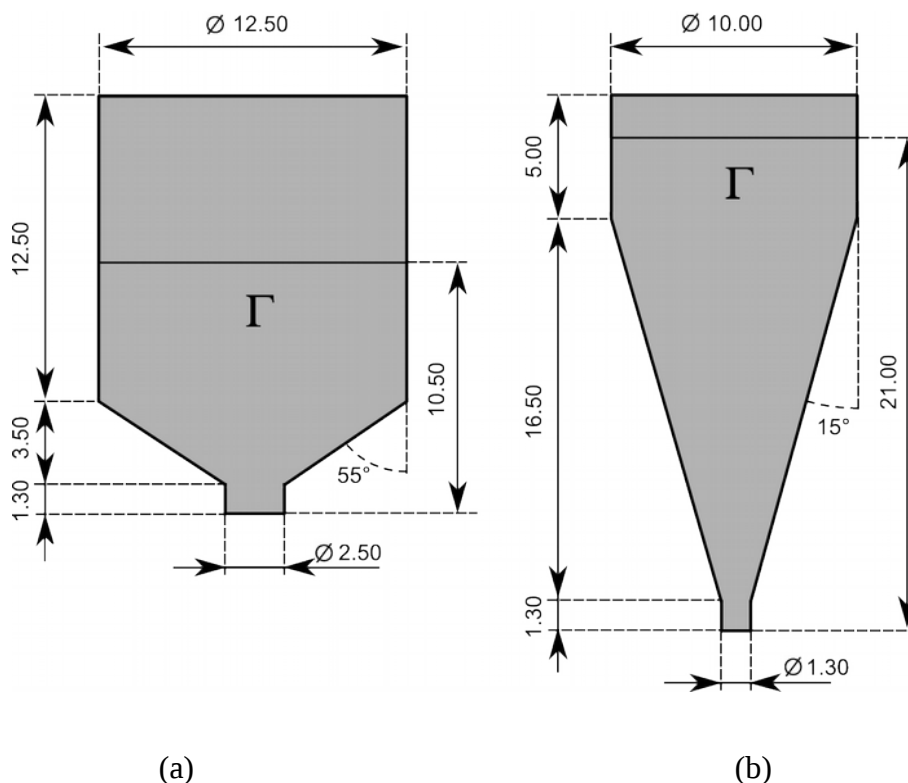

Figure 1. Silo geometries used in Ketterhagen *et al*. (2007) experiments, operating in (a) funnel flow regime and (b) mass flow regime. Γ indicates the initial interface between the two phases. The measures are given in cm.

The silos are filled with binary mixtures of glass beads; the level of filling is determined to load the same amount of material in both silos. The experiments use different loading policies. In this work, however, only the experiments starting from a homogeneous filling are considered.

The silos are discharged with a discontinuous start-stop method, following the ASTM Standard for evaluating the segregation propensity of the materials. 18 samples of 55 ml are withdrawn after each stop. The material collected in each sample is sieved to determine the mass fraction of each species. The experimental data from Ketterhagen *et al.* (2007), selected for model validation, include 2 types of regimes (mass and funnel flow), with mixtures of 2 different size ratios (1.9 and 4.3) and 3 different mass fractions (5, 20 and 50% of fines). Hence, a total of 12 experiments are simulated. Simulations have been carried out in 2D.

3.2 Experimental studies on tall silos

In the industrial practice silos have a longer cylindrical section, compared to those used by Ketterhagen *et al.* (2007) which follow the ASTM standard to measure segregation. To consider a more realistic configuration and study the interactions between the upper cylindrical and the lower conical section during segregation, the experiments by Arteaga and Tüzün (1990) are considered. They use two silos as well, made of Perspex, shown in Figure 2 with dimensions. The first one operates in funnel-flow regime (Figure 2a) and the second one in mass-flow regime (Figure 2b). These silos are loaded with a mixture of nearly spherical granules, made of ABS or acrylic particles, turnip and radish seeds. The mixtures initially loaded in silos are homogeneously premixed. Here we considered the experiments with mixtures of radish seeds and acrylic particles (see Table 1). Specifically, a mixture having 20% of fines with a coarse/fine diameter ratio equal to 4 was simulated.
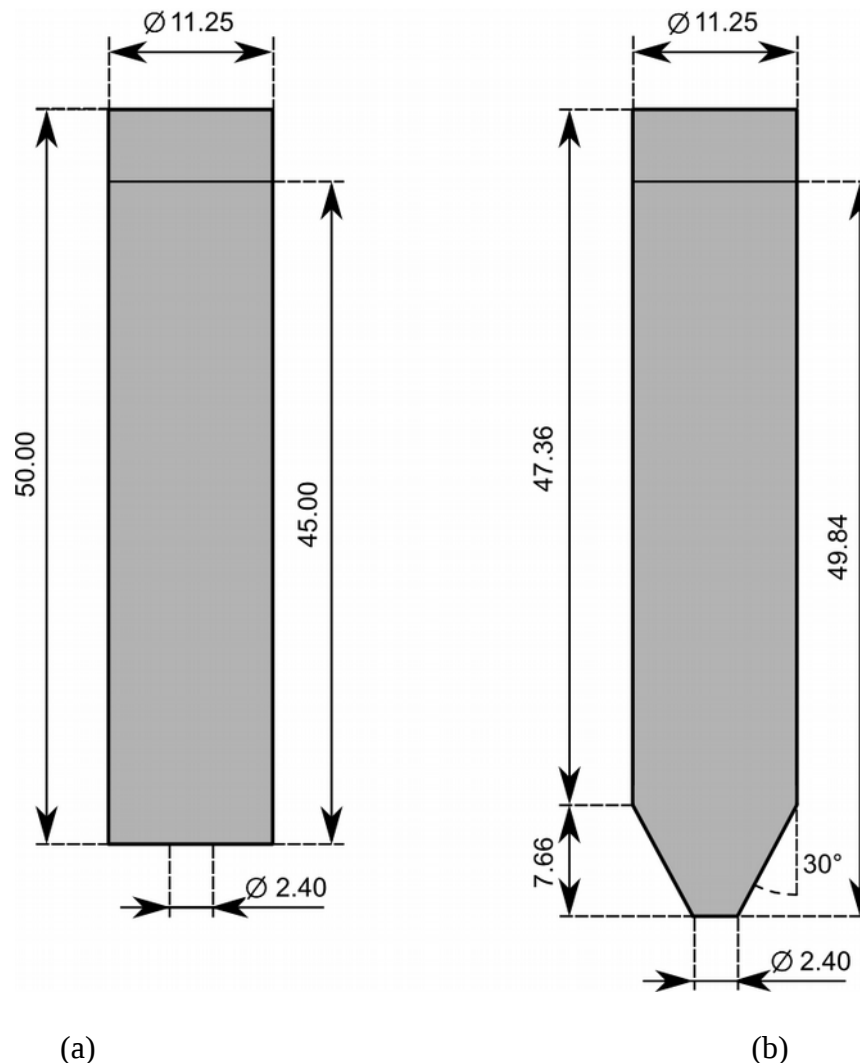

(a)   (b)

Figure 2. Silo geometries used in Arteaga and Tüzün (1990) experiments, operating in (a) funnel flow regime and (b) mass flow regime. Γ indicates the initial interface between the two phases. The measures are given in cm.

4. Results and discussion

4.1 Short silos

The evolution of uneven distribution of fines from initially uniform mixtures was simulated and shown in Figures 3 and 4, in case of funnel and mass flow, respectively. Conditions reflected the experiments of Ketterhagen *et al.* (2007). The time marks suggested that the segregation evolved quite rapidly. In funnel flow regime, Figure 3, the small particles accumulated below the shearing regions, shown in Figure 5. Shear concentrated below the free surface, particularly approaching the outlet; the material was mainly stagnant in the other regions of the hopper, close to the walls and the corners. The finest material migrated downwards where the shear was higher, then it remained trapped near the hopper wall.
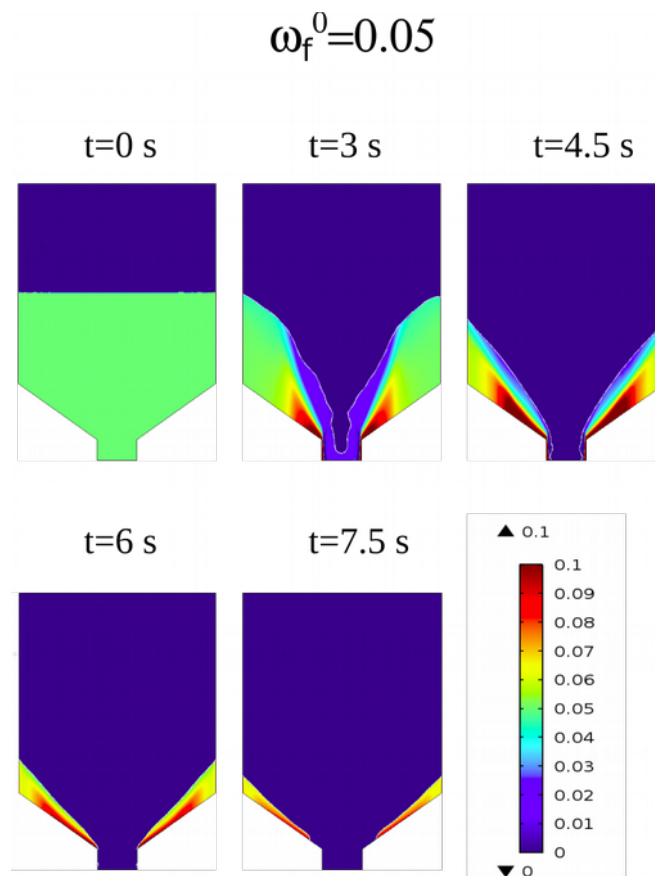

Figure 3. Evolution of segregation in funnel flow regime for $\omega_f° = 0.05$; $d_c/d_f = 4.3$. The color indicates the fines mass fraction.
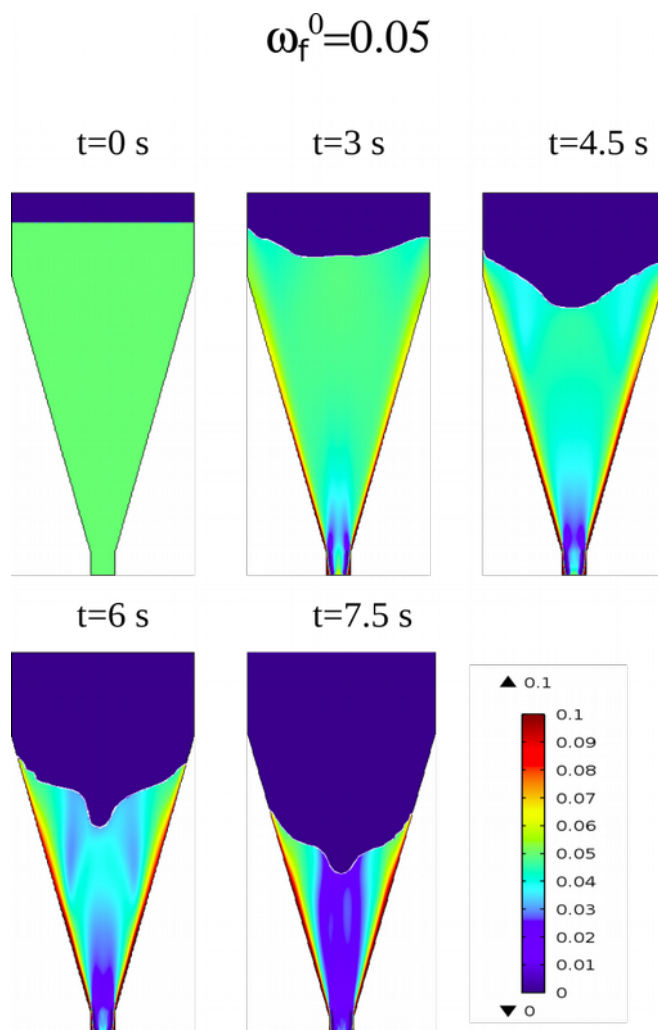
Figure 4. Evolution of segregation in mass flow regime for $\omega_f° = 0.05$; $d_c/d_f = 4.3$. The color indicates the fines mass fraction.

Since the nature of the funnel flow discharge is first in-last out, small particles rapidly accumulated in the hopper and they remained there until the end of discharge. This created an inhomogeneous outlet flow composition during time, where the coarse particles preferentially exited first.

On the contrary, mass flow, Figure 4, followed a first in-first out discharge pattern. The material was mainly sheared at the walls, as shown in Figure 6, contrary to the funnel flow where shear developed within the bulk (Figure 5). Fines accumulation occurred along the whole length of the inclined walls, where the shear was larger.
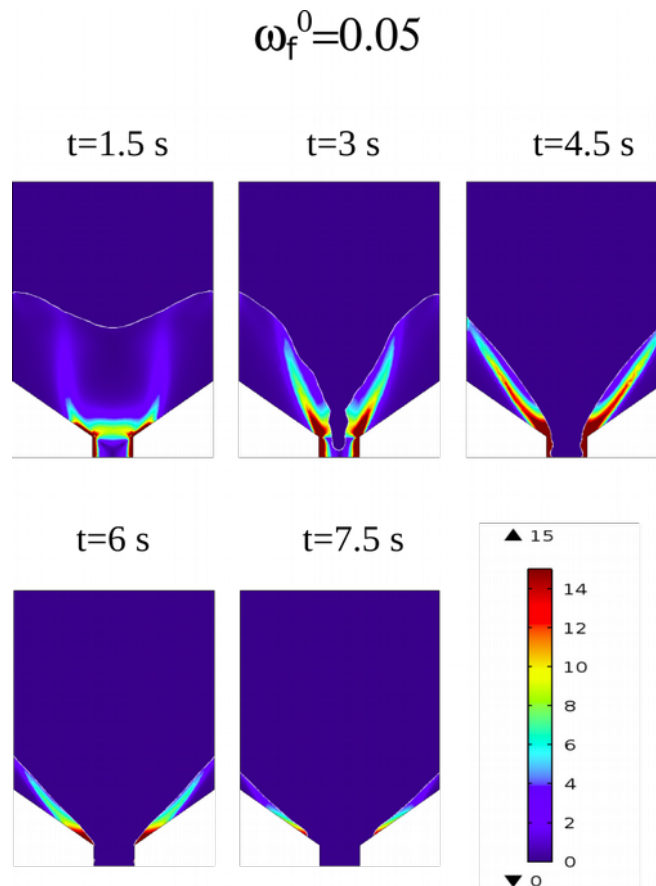
Figure 5. Evolution of shear rate [1/s] in funnel flow regime for $\omega_f^\circ = 0.05$; $d_c/d_f = 4.3$.

Segregation appeared to be less localized than in funnel flow regime, with a large core region that became almost devoid of fines. This was consistent with some shear to propagate throughout the whole hopper section (Figure 6), because of the converging flow, giving a chance for percolation of fines everywhere in the hopper. However, since all the material was flowing, including the most peripheral one, the average composition across the outlet section remained close to the initial value, even during the initial transient, when fines accumulated at the walls.

The composition maps shown in Figure 3 and 4 are intuitive and useful to understand the nature of the discharge mechanism and qualitatively visualize the effect of flow field on segregation. However, a more quantitative comparison is needed. It is formulated in the next section.

Mimicking the experimental procedure, we calculated the average composition in samples of fixed volume, collected at the outlet of the silo over discrete time intervals. Following the representation of the experimental results in the original literature, we reported the progress of discharge as normalized fines mass fraction (= fines mass fraction in each sample / initial fines mass fraction) vs. fractional mass discharged, up to a given time, for each experimental case analysed.
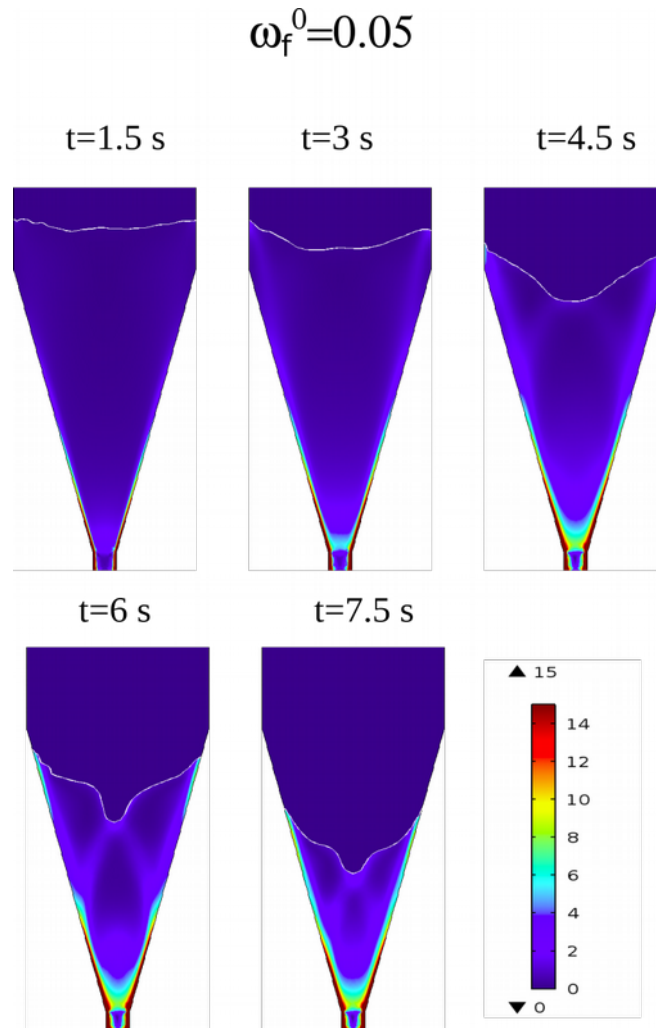
Figure 6. Evolution of shear rate [1/s] in mass flow regime for $\omega_f° = 0.05$; $d_c/d_f = 4.3$.

4.1.1 Tuning of the segregation flux

In this work the segregation process was modelled through the species material balance, where the transport mechanisms were convection and percolation.

Convection was ruled by the granular flow model, already validated in our previous works. The precise rheology of the granular materials in the experiments considered, could not be validated because neither the velocity, nor the stress fields inside the silos or at the walls are reported in the referenced literature. Still, we could successfully reproduce the discharge regime experimentally observed, either funnel or mass flow, at changing hopper geometry. This was a solid confirmation of the capability of our continuous granular flow model. Finally, the discharge velocity was always imposed in the experiments, further reducing the importance of a precise definition of the rheological parameters, as far as the flow regime was captured. It should be underlined that a good prediction of the local granular flow determined the accuracy of the segregation model, which was

affected by the local shear rate. It impacted on the segregation flux through eq. (9), where the relative importance of was ruled by $\frac{\partial \phi}{\partial t} + v \cdot \nabla \phi = 0$.

The segregation flux was proportional to the shear rate through a parameter K. However, a constant K led to predictions that were not sufficiently accurate, when compared to the experimental data, particularly in the funnel flow. It was observed that different values of K were required to fit the data satisfactorily when the initial amount of fines varied ($\tilde{\omega}_f$= 0.05, 0.2, 0.5). Optimal, constant K linearly correlated with $\tilde{\omega}_f$, as shown in Figure 7. The correlation recalls the findings of Hajra *et al.* (2012), that suggest a linear dependence of $K(\omega)$ with an intrinsic- and a concentration-dependent component, K_T and K_S, respectively, as in eq. (10).
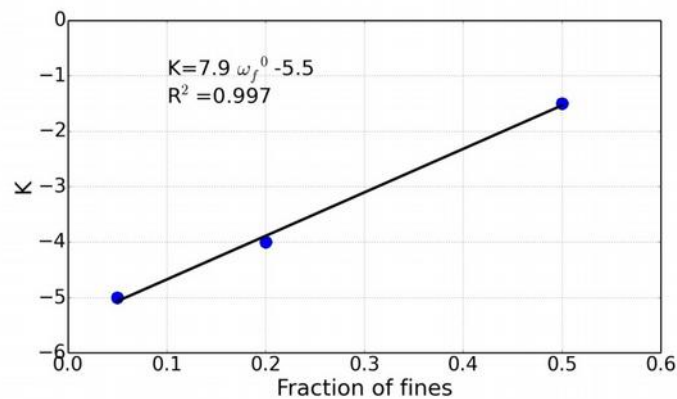

Figure 7. Optimal K values as a function of the initial fraction of fines.

The linear correlation found could be recast as $K = 2.4-7.9(1-\omega_f^0)$, which was consistent with eq. (10) when $K_T/d_c = 2.4$ and $K_S/d_c = -7.9$. Adopting these values of parameters K_T and K_S in eq. (10) to determine K as a function of the local composition, even if estimated from the initial, average composition, led to a good agreement between the predictions and the experiments, during all the discharge, as shown in Figure 8 for a single case. Others will follow.

The values of root mean square error, normalized with respect to the average value of the experimental fraction of fines (NRMSE), reported in Table 2, gave general information about the performance of the model.

Table 2. NRMSE for all tests in silos of Figure 1 for constant K and variable K.

System	Fine mass fraction	NRMSE [%] for constant K	NRMSE [%] for variable K
Funnel-flow 1.9-diameter ratio	0.05	10.1	10.4
	0.20	9.2	7.6
	0.50	7.4	4.2

Mass-flow 1.9-diameter ratio	0.05	8.7	8
	0.20	7.6	6.8
	0.50	6.7	3.9
Funnel-flow 4.3-diameter ratio	0.05	18.3	18.2
	0.20	9.7	9.6
	0.50	10.1	2.9
Mass-flow 4.3-diameter ratio	0.05	33.2	39.4
	0.20	20	11.4
	0.50	6.1	2.9

The implementation of the concentration-dependent K in eq. (8) gave a general improvement of results in most of the cases examined Enhancements were more significant with initial mixtures where fines were more abundant ($\omega_f^{\,0}$= 0.2 and 0.5). The NRMSE values, calculated considering concentration-dependent K, resulted less than 10%, except for some critical cases (d_c/d_f=4.3 and ω_f^0 = 0.05) that will be discussed later.
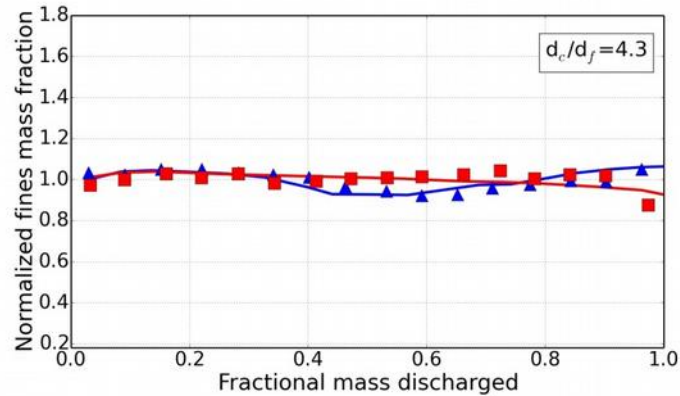

Figure 8. Comparison with experimental data of mass ($\triangleleft$) and funnel flow ($\square$) regimes in short silos after $K(\omega_f)$ optimization with ω_f^0 = 0.5; solid lines are numerical predictions.

4.1.2 The effect of the particle size ratio and initial fines concentration
In the first mixture analysed, the fines mass fraction was 0.05. Figure 9 shows the comparison between experiments and simulations for two different particle size ratios, d_c/d_f=1.9 and 4.3. As a general comment we observe that the extent of composition inhomogeneity at the outlet increased with the difference in the two particle sizes. For the largest particle size ratio, large voids were expected between the particles so that fines could percolate more easily, giving a greater tendency for the mixture to size segregate. The variations were larger in funnel flow compared to mass flow.

With the largest size ratio d_c/d_f=4.3, an excess of fines at the beginning of the discharge is reported in the literature experiments, both for mass and funnel flow (Figure 9b). It appears that even if the Authors try to start the discharge with a homogeneous mixture, it is impossible in practice to obtain such initial condition. The size ratio is so large that the small glass beads apparently percolate during silos loading, yielding an uneven initial mixture, before the material is set in motion. The difference in the initial composition between those assumed (i.e. implemented in the model) and those actually obtained experimentally weakened the validation, in the case of the largest size ratio. This was particularly evident for the mass flow regime. Clearly this represents a bias of the experimental data. After the initial phase, the qualitative trend was well reproduced by simulations and for the size ratio of 1.9 also a quantitative agreement with the experiments was obtained.
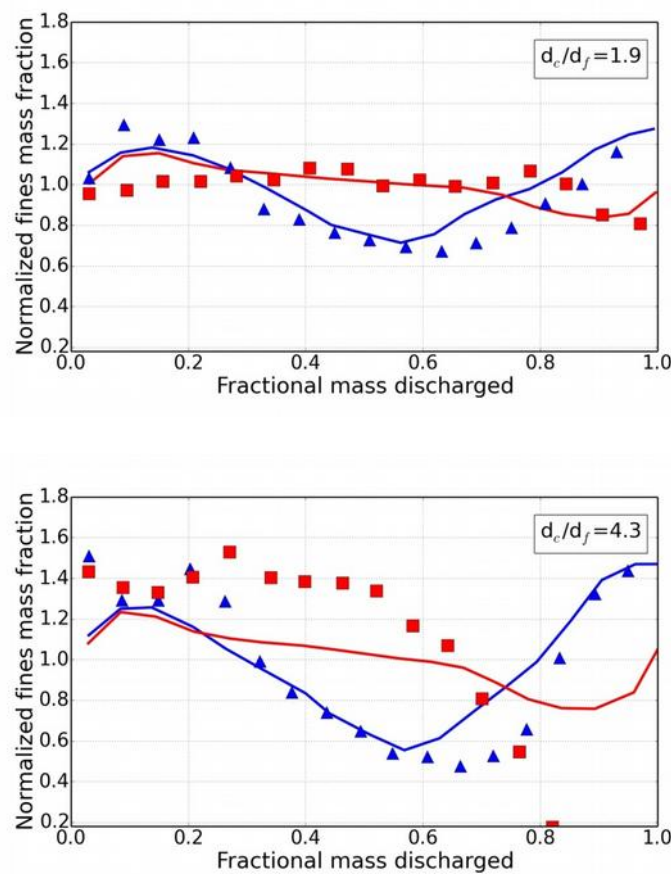

Figure 9. Comparison with experimental data of mass ($\triangleleft$) and funnel flow ($\square$) in short silos ω_f^0 = 0.05. ; solid lines are numerical predictions.

With a larger initial amount of fines, ω_f^0 = 0.2, the intensity of segregation decreased, as apparent from Figure 10. The qualitative agreement between numerical results and experimental data remained quite good, including some fluctuations of composition during the discharge, particularly in the case of funnel flow. As expected, for the largest size ratio the difficulty to experimentally

obtain an initially homogeneous composition is evident, jeopardizing the agreement with simulations for the mass flow regime.
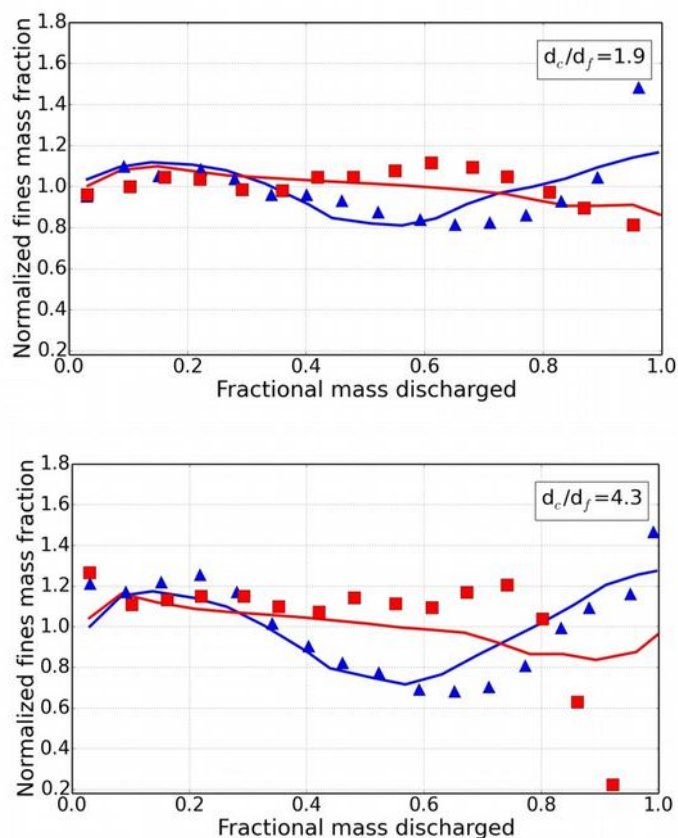

Figure 10. Comparison with experimental data of mass ($\triangleleft$) and funnel flow ($\square$) in short silos $\omega_f^0 = 0.2$; solid lines are numerical predictions.

However, for mass flow discharge and 4.3 diameter ratio the predictions were better than the more diluted case of $\omega_f^0 = 0.05$.

With a further increase of the initial amount of fines, $\omega_f^0 = 0.5$, the segregation dropped dramatically, as evident from Figure 11, in both flow regimes. This was well captured by the simulations. Contrary to what occurred in the previous cases, also the mixture with the larger particle size ratio remained homogeneous during the filling stage, and the numerical results were consistent with the initial phase of the discharge.
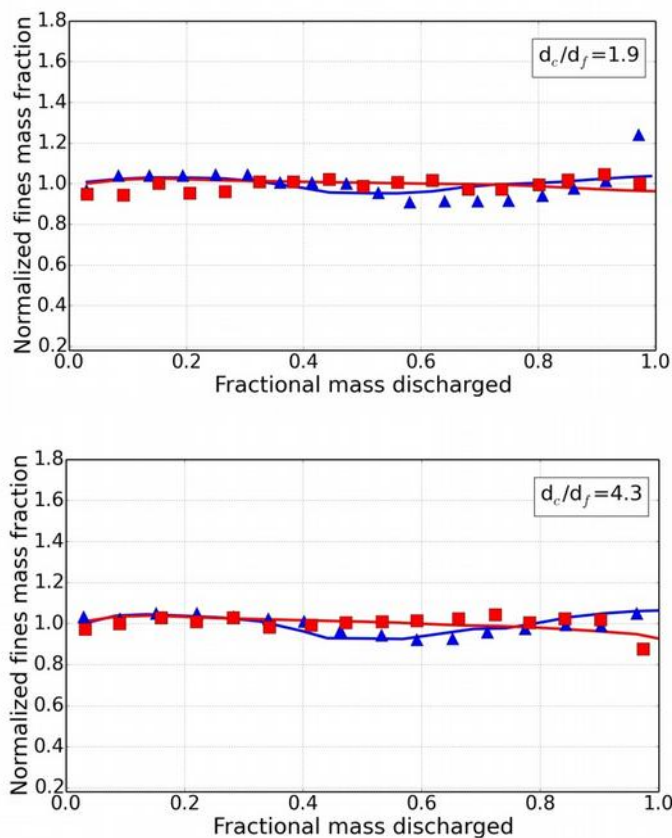
Figure 11. Comparison with experimental data of mass ($\triangleleft$) and funnel flow ($\square$) in short silos. ω_f^0 = 0.5; solid lines are numerical predictions.

The results of Figures 9 to 11 confirmed the qualitative observations suggested by the concentration maps, Figures 3 and 4. It could be observed that at the end of any funnel flow discharge, an increase of fines was observed at the outlet, more evident in the experimental data; this was not the case in the mass flow.

It was an expected consequence of the first in-last out nature of funnel flow; the residual portion of fines accumulated at the wall left the hopper towards the end of the discharge.

4.2 Tall silos

Tall silos experiments by Arteaga and Tüzün (1990) were used for comparison. We kept the same parameters (see Table 1) used for simulating the granular flow in short silo experiments, for consistency. Also the same $K(\omega_f)$ developed above for short silos was used for this configuration as well. We found that a constant linear dependence on $K = b d_r^2 \left| \frac{\partial c}{\partial y} \right|$ was adequate for short silos, while a stronger dependence, $\frac{1}{d_r} \frac{\partial c}{\partial y} \mu (1 - c) (1 - c) \left(\frac{c}{1-c} \right)^{-1}$, was required in tall silos, where the flow patterns were quite different.

Segregation was less intense than in short silos, as clear from Figure 12. However, there were quite significant deviations from the initial composition, particularly at the end of the discharge, that were well predicted by the model. Notwithstanding the crude choice of the parameters the agreement was good; the NRMSE values were always less than 10%, between 8.2 % and 7 %.

The experimental data suggested that three different stages could be identified during the discharge: an initial transient, a pseudo-steady state and a final transient. According to Arteaga and Tüzün (1990) the initial transient, with an enrichment of fines in the outlet flow is caused by the formation of a flame-shaped central core region, due to the granular bed dilation in the initial stages of the flow. In the dilated zone, percolation is favoured and accompanied by high value of shear rate in proximity of the outlet. The second stage, observed at 18% of the total discharge, is a pseudo-steady state in which no segregation is reported at the outlet. This is due to the absence of significant radial gradients of velocity in all the cylindrical section, except at the shear region adjacent to the walls. The third stage, finally, starts at approx. 78% of the discharge and is characterized by a larger segregation, greater in the funnel flow regime.

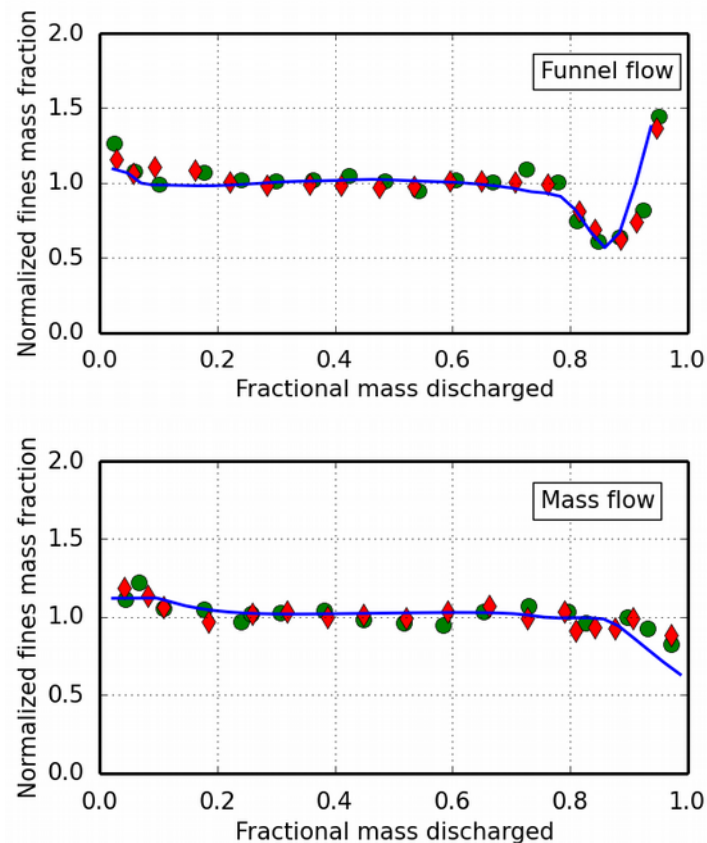**Figure 12**. Comparison with experimental data of funnel and mass flow regimes in tall silos $\omega_f°=$ 0.2. $d_c/d_f = 4$. Symbols ($\blacklozenge$, $\bullet$) are two replicas of the same experiment. The solid line is the numerical simulation.

Experiments and simulations showed that the segregation patterns on the short silos were similar to those observed in tall ones, in both discharge regimes, excepted for the absence of the pseudo-steady stage which was missing in short silos. All these stages were well captured by the simulations, thanks to a proper description of the segregation mechanism.

5. Conclusions

In this work segregation in granular flow of bi-dispersed mixtures was simulated, using a continuum approach. Granular flow was described with a rheological model for free-flowing materials and adapted to multi-phase and multi-component conditions. The simulation of bi-dispersed granular flow, allowing for a free, moving surface was achieved by an Eulerian, continuum approach to the two phase flow. Segregation was modelled with a mass transport equation applied to a bi-dispersed mixture of particles of different sizes. The model included the effects of two different mechanisms: advection due to flow and segregation due to percolation. Two different types of flow regime occurring in silos were investigated: the funnel and the mass flow regimes.

Simulations were compared with independent experimental data found in the literature, for short and tall silos. The simulations were carried out taking into account different size ratio (from 1.9 to 4.3) of the binary mixture and different initial fines concentration (from 5 to 50%). The segregation model, which primarily took into account the difference in size of the particles, was sensitive to the local mixture composition and the local shear rate, provided by the velocity field. The model was predictive for the spatial distribution of the mass fraction of the fines (or coarse) inside the silo at different stages of the discharge. Furthermore, it allowed to evaluate the fines weight fraction across the outlet with respect to the fractional mass discharged.

The segregation model proposed was simple and its strength was the coupling with a rheological model able to predict the flow rate and a model able to follow the interface between air and bi-dispersed solid. Notwithstanding the simplicity of the proposed segregation model and the crude estimation of the parameters, the qualitative and quantitative agreement with experimental data was good. In tall silos the model correctly predicted the three different stages of discharge: initial transient, pseudo-steady state and final transient.

Further work is however required to extend the model to more complex cases. These include additional percolation mechanisms originated by other physical properties such as differences in particle density and introducing inertial effects which typically occur at the free surface. Further refinements include considering poly-disperse systems, where different size classes are present. So far, we implemented a one-way coupling between the granular flow and the segregation model, where the flow structure affected the segregation, but the local composition did not modify the rheology. Further development is therefore required on the two-way coupling, to also take into account the effect of local size difference on the flow patterns.

Notation

d	=	particle diameter (m)
$\boldsymbol{g}$	=	gravity acceleration vector (m/s^2)
$\boldsymbol{J}_s$	=	vector of segregation flux (m/s)
K	=	segregation parameter (-)
K_S	=	intrinsic segregation parameter (-)
K_T	=	concentration-dependent segregation parameter (-)
k	○	dimensionless granular temperature scale parameter (-)
p	=	pressure (Pa)
$\boldsymbol{q}^T$	=	diffusive energy flux (Pa·m/s)
t	=	time (s)
$\boldsymbol{u}$	=	velocity vector (m/s)
v_s	=	segregation velocity (y-component) (m/s)
z^T	=	dissipation rate of mechanical energy (Pa/s)

Greek letters

$\dot{\gamma}$	=	magnitude of shear rate (1/s)
η	=	viscosity (Pa·s)
	=	parameter in the viscosity coefficient (1/s)
θ	=	granular temperature (m^2/s^2)
θ^*	=	granular temperature scale (m^2/s^2)
$\boldsymbol{\Pi}$	=	deviatoric stress tensor (Pa)
ρ	=	density (kg/m^3)
ϕ	=	volume fraction (-)
ω	=	mass fraction (-)

Sub- and superscripts

0	=	initial
f	=	granular material fine component
c	=	granular material coarse component
a	=	air
g	=	granular

References

Arteaga P., Tüzün U. (1990). Flow of binary mixtures of equal-density granules in hoppers – size segregation, flowing density and discharge rates. *Chemical Engineering Science*, **45**, 205-223.

Artoni R., Santomaso A., Canu P. (2009). Simulation of dense granular flows: dynamics of wall stress in silos. *Chemical Engineering Science*, **64**, 4040-4050.

Artoni R., Zugliano A., Primavera A., Canu P., Santomaso A. (2011). Simulation of dense granular

flows: comparison with experiments. *Chemical Engineering Science*, **66**, 548-557.

ASTM Standard practice for measuring sifting segregation tendencies of bulk solids, D 6940-03 (2003).

Barker G. C., Metha A. (1993). Transient phenomena, self-diffusion, and orientational effects in vibrated powders. *Physical Review E*, **47**, 184-188.

Bridgwater J. (1994). Mixing and segregation mechanisms in particle flow. In: *Granular matter: an interdisciplinary approach* (Metha A., Ed.), Springer-Verlag, New York (U.S.A.) pp.161-193.

Brown, R. L. (1939). The fundamental principles of segregation. *Journal of the Institute of Fuel*, **13**, 15.

Christakis N., Chapelle P., Strusevich N., Birdle I., Baxter J., Patel M. K., Cross M., Tüzün U., Reed A. R., Bradley M. S. A. (2006). A hybrid numerical model for predicting segregation during core flow discharge. *Advanced Powder Technology*, **17**, 641-662.

Christakis N., Patel M. K., Cross M., Baxter J., Abou-Chakra H., Tüzün U. (2002). Predictions of segregation of granular material with the aid of physica, a 3-d unstructured finite-volume modelling framework. *International Journals for Numerical Methods in Fluids*, **40**, 281-291.

Cundall P.A., Strack D.L. (1979). A discrete numerical model for granular assemblies. *Géotechnique*, **29**, 47-65.

Dolgunin V. N., Kudy A. N., Ukolov A. A. (1998). Development of the model of segregation of particles undergoing granular flow down an inclined chute. *Powder Technology*, **96**, 211-218.

Fan Y., Schlick C. P., Umbanhowar P. B., Ottino J. M., Lueptow R. M. (2014). Modeling size segregation of granular materials: the roles of segregation, Advection and Diffusion. *Journal of Fluid Mechanics*, **741**, 252-279.

Gray J. M. N. T., Thornton A. R. (2005). A theory for particle size segregation in shallow granular free-surface flows. *Proceedings of the Royal Society A*, **461**, 1447-1473.

Hajra S. K., Shi D., McCarthy J. J. (2012). Granular mixing and segregation in zigzag chute flow. *Physical Review E*, **86**, 061318.

Henann D.L, Kamrin K.A. (2013). Predictive, size-dependent continuum model for dense granular flows. *Proceedings of the National Academy of Sciences.* **110**, 6730-6735.

Jenkins J. T., Savage S. B. (1983). A theory for the rapid flow of identical, smooth, nearly elastic particles. *Journal of Fluid Mechanics*, **130**, 187-202.

Ketterhagen W. R., Curtis J. S., Wassgren C. R., Kong A., Narayan P. J., Hancock B. C. (2007). Granular segregation in discharging cylindrical hoppers: a discrete element and experimental study. *Chemical Engineering Science,* **62**, 6423-6439.

Knight J. B., Jaeger H. M., Nagel S. R. (1993). Vibration-induced size separation in granular media: the convection connection. *Physical Review Letters*, **70**, 3728-3731.

Marks B., Einav I., Rognon P. (2011). Polydisperse segregation down inclines: towards degradation models of granular avalanches. in: *Advances in Bifurcation and Degradation in Geomaterials*, (Bonelli S., Dascalu C., Nicot F., Eds.), Springer Netherlands, Dordrecht (Netherlands) pp. 145-

151.

May L. B. H., Golick L. A., Phillips K. C., Shearer M., Daniels K. E. (2010). Shear-driven size segregation of granular materials: modeling and experiment. *Physical Review E*, **81**, 051301.

Neddermann R. M. (1992). Statics and kinematics of granular materials, Cambridge University Press.

Olsson E., Kreiss G. (2005). A conservative level set method for two phase flow. *Journal of Computational Physics*, **210**, 225-246.

Savage S. B (1998). Analyses of slow high-concentration flows of granular materials. *Journal of Fluid Mechanics*, **377**, 1-26.

Santomaso A. C., Olivi M., Canu P. (2004) Mechanisms of mixing of granular materials in drum mixers under rolling regime *Chemical Engineering Science*, **59** (16), 3269-3280.

Santomaso A. C., Petenò L., Canu P. (2006) Radial segregation driven by axial convection *Europhysics Letters*, **75** (4), pp. 576-582.

Savage S. B (1998). Analyses of slow high-concentration flows of granular materials. *Journal of Fluid Mechanics*, **377**, 1-26.

Savage S. B., Lun C. K. K. (1988). Particle size segregation in inclined chute flow of dry cohesionless granular solids. *Journal of Fluid Mechanics*, **189**, 311-335.

Shi D., Abatan A. A., Vargas W. L., McCarthy J. J. (2007). Eliminating segregation in free-surface flow of particles. *Physical Review Letters*, **99**, 148001.

Sleppy J. A., Puri V. M. (1996). Size-segregation of granulated sugar during flow. *Transactions of the ASAE*, **39**, 1433-1439.

Taberlet N., Newey M., Richard P., Losert W. (2006). On axial segregation in a tumbler: an experimental and numerical study. *Journal of Statistical Mechanics: Theory and Experiment*, **07**, P07013.

Volpato S., Artoni R., Santomaso A. C. (2014). Numerical study on the behavior of funnel flow silos with and without inserts trough a continuum hydrodynamic approach. *Chemical Engineering Research and Design*, **92**, 256-263.

Williams J. C. (1963). The segregation of powders and granular materials. *Fuel Society Journal (University of Sheffield)*, **14**, 29-34.